Proceedings World Geothermal Congress 2010
Bali, Indonesia, 25-29 April 2010

# Aluminum Alloy Drill Pipe in Geothermal Drilling

Erin R. Anderson
980 South Ogden St. Denver, CO 80209
Erin.anderson@res.is

**Keywords:** Aluminum, Drill Pipe, Geothermal, Drilling, ADP, temperature model.

## ABSTRACT

The purpose of this investigation is to determine the application opportunities of aluminum alloy drill pipe (ADP) in geothermal drilling environments. With the improved development into ultra high energy extraction regions, the geothermal drilling industry is under high demand and is being tested to drill deeper, faster, and at reduced costs in order to make geothermal competitive economically and to satisfy energy demands. The achievement of greater drilling depths requires the advancement of the drilling industry to address limitations in the weight capacity of the drill rigs and the temperature limitations of the drilling components. Aluminum alloy drill pipes (ADP), sometimes referred to as Lightweight Aluminum Drill pipes (LADP) have been used in the drilling industry in Russia for many years. Due to ADP's lightweight and high strength to weight ratio there are several advantages over conventional steel pipe. These advantages include the use of larger diameter drill pipe with thicker walls which increase annular flow; reduced pressure loss inside the drill pipe, resulting in smaller pump requirements; reduced derrick loads and hook loads due to reduced weight per length compared to steel and increased buoyancy effects in drilling fluids, resulting in smaller rigs or greater depth penetrations with current rigs; and reduced stresses in a number of drilling design parameters. The application ranges of ADP utilization was studied in regards to temperature limitations, critical buckling loads and strength of materials, geothermal fluid chemistry, drilling fluid pressure losses and hydraulics, load comparisons, tool joint bonding, and economical cost analysis.

## 1. INTRODUCTION

The geothermal industry is having to drill deeper for both conventional hydrothermal reservoir and for Enhanced Geothermal Systems (EGS formally known as Hot Dry Rock (HDR) systems) to generate substantial base load power and achieve economies of scale with larger power plants. This is where aluminum alloy drill pipe can become a benefit. ADP can allow smaller drilling rigs to achieve greater depths without sacrificing drilling performance and rate of penetration.

While ADP is new to the geothermal industry, Russia has been extensively using ADP since the 1960's. ADP was widely used in the USSR in the 1960's and 70's and represented nearly 50% of the drill pipe in use. The tool joint connections were not satisfactory and as drilling depths increased, the tool joints on ADP began to cause a number of failures. This resulted in steel drill pipes securing 85% of total drill pipe in use until Russia undertook the Kola ultra deep drilling project, which took place from 1970 until its completion in 1983 (Gelfgat et al. 2003). As a result of the greater depth goals (goal of 15,000 meters) and the limitations of drill rig hook loads, ADP was revitalized with more secure steel tool joints (Chesnokov 2008). Currently, more than 120,000 meters of ADP are being used in Russia and Western Siberia. The supply of ADP and its continued engineering has been mostly due to Aquatic Company, Russia's premier aluminum alloy product fabricator and supplier. As a result, "the experience of Aquatic Company in development, production and use of ADP became the basis for international standard ISO 15546 'Aluminum alloy drill pipe for use in petroleum and natural gas industries', which was put in force in 2003" (Aquatic Company 2008).

There are many advantages to aluminum alloy drill pipe (ADP) that can improve the drilling operations and reduce costs. The weight per meter of ADP without tool joints is half that of steel and with tool joints ADP is approximately 58% the weight per meter of steel, which results in reduced derrick and hook loads. Hook loads are also reduced as a result of the reduced drag forces from the reduced weight of ADP. This can result in smaller drill rigs being used to drill deeper wells. The lighter alloy pipe also allows for the use of larger diameter pipe with greater thickness, uncompromising the strength compared to steel. The larger diameter drill pipe reduces the area of the annulus thereby increasing velocities and decreasing pressure losses inside the drill pipes. This reduces the drilling fluid pump requirements thereby saving capital and fuel costs. The reduced weight also improves the buoyancy effect of ADP which in a 10 lb/gal mud (1.19826 g/cm3) has been shown to be about half the weight in air. This reduces the axial and bending stresses, allowing higher-angle doglegs to be drilled more safely.

Although the advantages are impressive there are limitations of ADP; with a high coefficient of thermal conductivity compared to steel, problems will arise with the stability of the ADP at high temperatures; the decreased weight reduces the burst strength and buckling loads of the drill pipe. In order for the geothermal drilling industry to reduce costs, maximize drill rig efficiency, achieve greater drilling depths than ever before, and reduce the overall drilling time, the use of aluminum alloy drill pipes are one solution. The benefits, limitations, and application ranges for ADP need to be established to accurately determine its use in the geothermal drilling industry.

## 2. TEMPERATURE MODEL

In order to determine the application range of aluminum drill pipe in a geothermal borehole, a temperature model was developed to generate bottom hole temperature for a standard geothermal borehole using ADP. The heat transfer and temperature model was developed in Excel to simulate the heat transfer from the formation to the annulus and from the annulus through the drill pipe to the fluid in the drill pipe. In thermodynamic terms this is a very complicated system. Without simplifying the elements, this would be a non-Newtonian fluid – because drill mud does not have the same viscous properties as water – (Bourgoyne et al. 1991, Moore 1986, Santoyo et al. 2003), turbulent flow, single pass counter-flow heat exchanger that is not insulated and has a varying heat flux to the "surroundings" along the length of the pipe (i.e. at one end of the heat exchanger the surroundings is hotter than the fluid in the pipes and at the other end could be cooler).

This model was based on the STAR model, developed by Mr. Sverrir Thórhallsson and Dr. Árni Ragnarsson at Iceland GeoSurvey (ISOR) and as presented in Huang Hefu's UNU report (2006). While the basic premise behind this model follows the STAR model, there have been several changes made to the approach of certain values and in several equations.

This model will focus on the direct circulation method. The temperature is known at the standpipe, $T_s$ [°C], and is assumed to be the same temperature as at the top of the drill pipe at a depth of zero (0) meters. The temperature of the drilling fluid flowing down the inside of the drill pipe, $T_t$ [°C], will increase as the depth increases, and is influenced by the heat transfer coefficient of the drill pipe and the temperature of the annulus at that depth in the well. The annulus temperature, $T_a$ [°C], reduces as the drilling fluid flows up the annular space in the borehole. The temperature in the annulus is affected by the formation temperature and the cooling fluid inside the drill pipe. The temperature of the annulus and the drill pipe fluid are assumed to be equal at the bottom of the borehole. The well will be divided into hundreds or thousands of cells depending on the depth interval chosen, dz [m], and the depth of the well, z [m], being analyzed. Within each cell the properties of the fluid are assumed to be constant. Figure shows a schematic of the wellbore temperature model parameters.

The model is set up to take an "educated" guess of the temperature at the bottom of the borehole, $T_t$ at the total depth of wellbore and then optimizes this bottom borehole temperature value, and the temperature of subsequent cells to the surface of the wellbore so that the temperature calculated at the top of the inside of the drill pipe, $T_t$ at the depth=0, is equal to the surface temperature in the standpipe, $T_s$.

The temperature gradient in the radial direction (the change in temperature as a function of distance in the horizontal direction) is much greater than the vertical temperature gradient from cell to cell (Chugunov et al. 2003, Fomin et al. 2005). This is especially true in turbulent flow conditions which are characterized by rapid heat dispersion perpendicular to the flow (Bird et al. 2002). Therefore the heat in each cell is calculated by "assuming horizontal heat conduction in an adjacent rock formation" to the annulus, continuing through the drill pipe to the drilling fluid in the center pipe (Kanev et al. 1997, p. 332). The heat flow from the rock formation to the annulus is dependent on the temperature of the rock at that depth and the circulation time (the time the drilling fluid has been flowing through a cell). In other words, this model does not assume that the bore-face temperature is constant but rather changes with time and depth as is more realistic. The varying bore-face temperature has been an oversight of several other wellbore simulators, which has been criticized by Fomin and Chugunov (2005, 2003). The circulation time will vary for each wellbore based on the total number of drilling days and the depths achieved each day. In this model, the time function can be estimated as a linear function based upon the total number of drill days at depth zero down to 1 day of fluid circulation at the bottom of the wellbore. Similarly, this model allows for actual input of wellbore cooling data and is designed to interpolate between entered data and will therefore linearize between points. If temperature logs of the location of the wellbore are not available for input into the model, the formation temperature will be assumed to follow the boiling point with depth curve (BPD). Similarly to the cooling data, if formation temperature is input, the temperature for a certain depth will linearize between points.

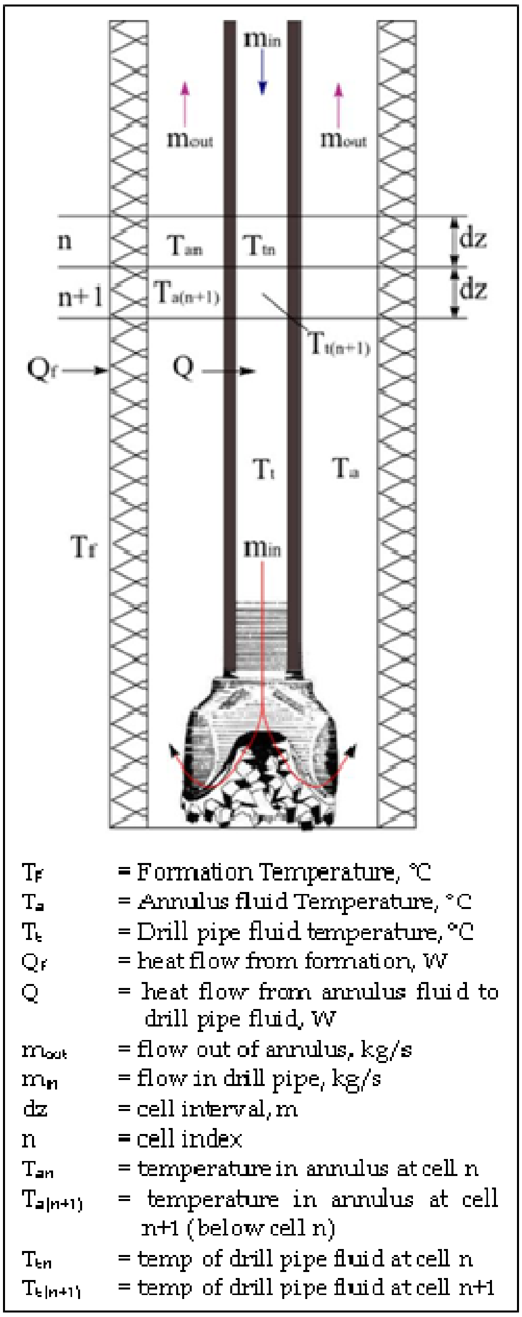


**Figure 1: Temperature Model Wellbore circulation system.**

## 3. STRENGTH OF MATERIALS OF PIPE

Drill string components undergo various combinations of stresses and strains in order to achieve the end goal of deep underground resource recovery. The structural analysis of the drill pipe is critical to the application of aluminum alloy drill pipe in the geothermal industry. The structural properties of aluminum alloy and steel were calculated for the following forces and physical affects were compared to the yield strength for increasing temperature: Tension Forces in Drill pipe; Axial Yield Strength; Compression – Buckling; Internal Yield Pressure – Bursting; Collapse; Elongation and Stretch; Bending; Torsion; Fatigue;

Corrosion; Hydraulic and drag forces. Several grades of steel and aluminum pipes were analyzed. Table 1 and Table 2 below show the grades and compositions of materials for the drill pipes.

One of the most important parameters is the yield strength versus temperature for each steel grade or aluminum alloy. The yield strength of aluminum decreases more rapidly than steel as the temperature increases. Table 3 below shows the tensile yield strength versus temperature for each grade analyzed. The steel grades represent three of the four API steel drill pipe grades. The API S-135 is the strongest of the steel drill pipe available. The E-75 was the most frequently used in the geothermal drilling but due to its limited availability, geothermal drilling contractors have replaced it with G-105. The aluminum alloys were selected based on their current availability, such as that of 2024 (D16) as used in Russia, and two alloys currently offered from Alcoa, the 2014 and 7055. Although the exposure time greatly differs between the steel and aluminum alloys, the tensile properties versus temperature of numerous low-alloy grade steels were researched and the results showed that the values presented in Table 3 below and shown graphically in Figure 2 correspond to other steels in terms of percent reduction from room temperature yield strength.

**Table 1: Aluminum Drill Pipe Alloy and Composition.**

| | | **Aluminum Chemical Compositions Limits** | | | | | | | | | |
|---|---|---|---|---|---|---|---|---|---|---|---|
| | | % of weight | | | | | | | | | |
| Alloy | Equivalent Comp. | **Si** | **Fe** | **Cu** | **Mn** | **Mg** | **Cr** | **Ni** | **Zn** | **Ti** | **Al** |
| 2024 | D16T | 0.5 | 0.5 | 3.8-4.9 | 0.3-0.9 | 1.2-1.8 | 0.1 | | 0.25 | 0.15 | Remainder |
| 2014 | | 0.5-1.2 | 0.7 | 3.9-5.0 | 0.40-1.2 | 0.2-0.8 | 0.1 | | 0.25 | 0.15 | Remainder |
| C405 | 7055 | 0.1 | 0.15 | 2.0-2.6 | 0.05 | 1.8-2.3 | 0.04 | | 7.6-8.4 | 0.06 | Remainder |
| 7014 | | 0.5 | 0.5 | 0.3-0.7 | 0.3-0.7 | 2.2-3.2 | | 0.1 | 5.2-6.2 | | Remainder |

(The Aluminum Association 2006)

**Table 2: Steel Drill Pipe Grade and Material Composition.**

| | | **Steel Chemical Compositions** | | | | | | | | |
|---|---|---|---|---|---|---|---|---|---|---|
| | | % of weight | | | | | | | | |
| Alloy | Equivalent Comp. | **Si** | **Fe** | **C** | **Mn** | **P** | **Cr** | **Ni** | **Mo** | **S** |
| API S-135* | | 0.39 | balance | 0.33 | 1.07 | 0.022 | 0.89 | 0.33 | 0.21 | 0.01 |
| API E-75** | | | | | | <0.03 | | | | <0.03 |
| API G-105** | | | | | | <0.03 | | | | <0.03 |

*(Miscow et al. 2004) **API Spec 5D standard

**Table 3: Temperature vs. Yield Strength of Steel and Aluminum Drill Pipe Grades.**

| | d | | | f Data read from graph of % of Room Temp Yield Strengh vs. Temp for AISI Low-Alloy Steel | | |
|---|---|---|---|---|---|---|
| | **2014-T6** | **7055** | **2024-T4** | **E 75 Steel** | **G 105 Steel** | **S 135 Steel** |
| | 10,000 hour exposure to temperatures | | | 0.5 hour exposure to tempertures | | |
| Temp °C | Yield MPa | Yield MPa | Yield MPa | Yield MPa | Yield MPa | Yield MPa |
| -195 | 495 | 615 | 420 | | | |
| -80 | 450 | 540 | 340 | 553 | 775 | 996 |
| -30 | 425 | 525 | 325 | 538 | 753 | 968 |
| 25 | 415 | 505 | 325 | 517 | 724 | 931 |
| 100 | 395 | 440 | 310 | 491 | 688 | 884 |
| 150 | 240 | 185 | 250 | 470 | 659 | 847 |
| 205 | 90 | 85 | 130 | 450 | 630 | 810 |
| 260 | 50 | 60 | 60 | 429 | 601 | 773 |
| 315 | 34 | 48 | 41 | 408 | 572 | 735 |
| 370 | 24 | 38 | 28 | 383 | 536 | 689 |

[d] The Aluminum Association 2006b [f] Metallic Materials Properties Development and Standardization 2008

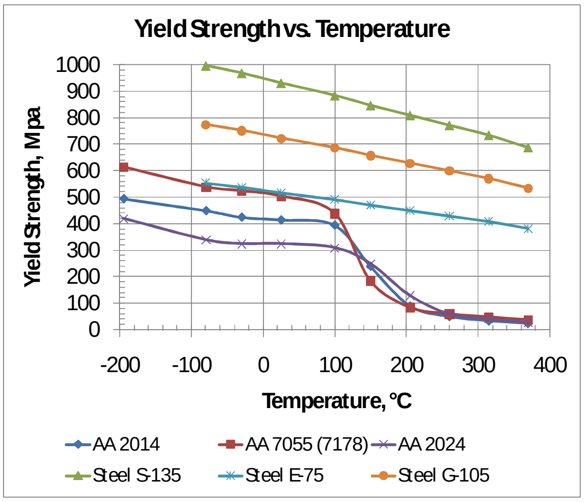


**Figure 2: Yield Strength versus Temperature for AA and API steel grades.**

### 3.1 Bending Stress in Dogleg

The equation used to calculate the bending stress in a curved borehole, includes the axial force exerted due to drill pipes hanging below the point of interest and therefore the axial force does not need to be added to the stress. The maximum bending stresses in the drill pipe can be calculated using the angle of the dogleg severity (DLS), α by Lubinski's formula (Bourgoyne et al. 1991, Rahman et al. 1999, Vaisberg et al. 2002) show in.

$$\sigma_b = \left( \frac{E d_{po} C L_{b2j} \sqrt{\frac{F_{ten}}{EI}}}{2 \tanh \left[ L_{b2j} \sqrt{\frac{F_{ten}}{EI}} \right]} \right) \qquad (1)$$

$\sigma_b$ = Bending Stress [psi, Pa]

$d_{po}$= nominal outside drill pipe diameter [in, m]

E= Modulus of Elasticity of pipe material [psi, Pa]

C= Dogleg severity.

$$C = \left( \frac{\alpha}{\text{length between measured angles}} \right) 100\,ft[\text{rad}/100\text{ft}]$$

$$C = \left( \frac{\alpha}{\text{length between measured angles}} \right) 30m[\text{rad}/30\text{m}]$$

A= Dogleg severity angle [°] or [radian], if in degrees multiple by (π/180)

$$A = \cos^{-1}\left[ (\cos i_1)(\cos i_2) + (\sin i_1)(\sin i_2)(\cos(A_2 - A_1)) \right]$$

$i_{1,\dots n}$ = drift angle measured from vertical or inclination angle [°]

$A_{1,\dots n}$ = azimuth angle [°]

$L_{b2j}$ = half the length of the drill pipe (distance between two joints) [in, m]

$F_{ten}$ = Axial tension force [psi, Pa]

I = Moment of Inertia of the cross section of the drill pipe body [$in^4$, $m^4$]

In this case, the pipe at the top of the build-up section is being analyzed since it is the critical pipe in the dogleg. It should be noted that the DLS is computed based on 30 meter lengths (ie. α/30m). The results are tabulated in Table 4.

**Table 4: Drill Pipe Bending Stresses in a 3000 meter hole with an Dogleg Severity (DLS) of 1.4°/30m.**

| ***Bending*** | **Stl 5" S 135** | **Stl 4.5" S 135** | **Stl 5" E75** | **Stl 5" G105** | **Al 6 5/8" 2024-T4** | **Al 5" 2014-T6** | **Al 5" 7055** |
|---|---|---|---|---|---|---|---|
| MPa | 42.0 | 42.6 | 40.7 | 41.5 | 16.5 | 17.1 | 17.0 |

Clearly, the ADP undergoes significantly less stress through the same dogleg as the steel pipe. This is due in large part to the smaller modulus of elasticity and the reduced tensile load on the aluminum drill pipe as a result of the lighter density as compared to steel. Also, there are reduced bending stress advantages for aluminum pipes as the diameter gets bigger. The bending stresses are far below the yield strength for all temperatures up to 300°C. These bending stresses neglect the torsional stress, fluid pressures, and fatigue stresses.

### 3.2 Pressure Losses

One of the main advantages of ADP is its reduced weight in addition to its increased specific strength (strength-to-weight ratio) as compared to steel. This allows thicker and larger diameter pipes which have lower bending stress in doglegs and improved hydraulics in the wider diameter geothermal wells as compared to oil and gas wells. The total pressure losses are shown in Table 5. The pressure losses depend on the pipe dimensions which reduced the number of pipes analyzed to four. The pressure losses in mud (a Non-Newtonian fluid) and water (a Newtonian fluid) were both calculated to compare the pressure losses and subsequent costs from the total pump power required for each pipe sample. The pump power requirements that were calculated are summarized in Table 6.

**Table 5: Total Pressure Drop in Wellbore.**

| **Total Pressure Drop** | **Steel Drill Pipe** | | **Aluminum Drill Pipe** | |
|---|---|---|---|---|
| | Steel 5" | Steel 4.5" | AA 6 5/8" | AA 5" |
| | kPa | kPa | kPa | kPa |
| Newtonian | 16462 | 23500 | 9037 | 18712 |
| Non-Newtonian | 15581 | 22035 | 8772 | 17644 |

**Table 6: Pump Power Required Based on Pressure Losses.**

| **Pump Power Required** | **Steel Drill Pipe** | | **Aluminum Drill Pipe** | |
|---|---|---|---|---|
| | Steel 5" | Steel 4.5" | AA 6 5/8" | AA 5" |
| | kW | kW | kW | kW |
| Newtonian | 823 | 1175 | 452 | 936 |
| Non-Newtonian | 779 | 1102 | 439 | 882 |

The graph below in Figure 3 shows the pressure losses throughout the drill pipe. The pressure losses start in the surface equipment. The pressure decreases due to losses as the drilling fluid flows down the drill pipe and drill collar, through the mud pump and drill bit, and up the annulus back to the surface.

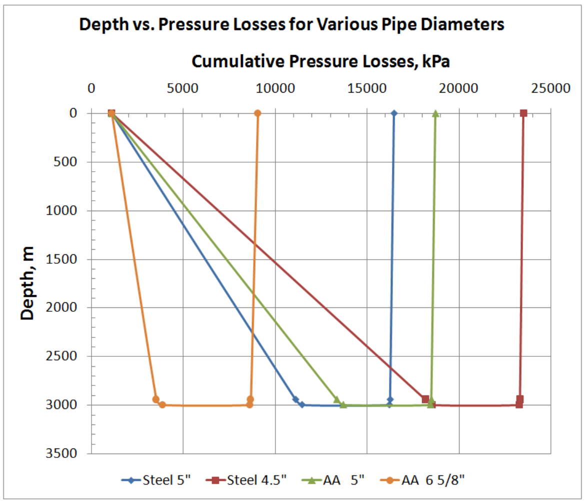


**Figure 3: Depth versus Pressure Losses of Drilling Fluid Circulation.**

The results of the calculations show that there are advantages to using larger diameter pipes since the pressure losses for both Newtonian and non-Newtonian drilling fluids are reduced and the total pump power is reduced as well.

### 3.3 Corrosion of Aluminum Alloys

The corrosive environments of geothermal reservoir and wellbores differ globally from location to location. Sometimes even wells within kilometers of each other can have significantly different chemical compositions. The severity of the corrosive nature of a geothermal fluid is drastically different from region to region. However, due to current drilling techniques which include over pressurizing the wellbore relative to the surrounding reservoir pressure and the nature of the drilling fluids, the interaction of geothermal fluid mixing with drilling fluid can be avoided if maintained properly. Therefore, the drill pipes are typically only exposed to the drilling fluid, which is regulated with depth by composition and pH, ranging from pH 7 to pH 10.

However, unlike steel drill pipes, aluminum alloys have the unique ability to form a protective oxide film on the pipe, which protects them from further environmental damage. The view of 'corrosion' is debatable. Some might view the oxide film, which is strongly bonded to the pipe surface as a form of corrosion. But if the pipe is damaged, the oxide film "re-forms immediately in most environments" and "on a surface freshly abraded and then exposed to air, the barrier oxide film is only 1 nm thick but is highly effective in protecting the aluminum from corrosion" (Hollingsworth & Hunsicker 1997, p. 1427).

It an article by Chesnokov (2008), he reports that ADP undergoes zero corrosion in aggressive environments and that "a year- long operation in hydrogen sulfide usually destroys any steel pipe, whereas aluminum just becomes black covered with an oxide film".

One of the important factors affecting alloys and their corrosive resistive behavior is the other metals in the alloy material composition. Due to the "electrochemical nature of most corrosion processes, relationships among solution potentials of different aluminum alloys, as well as between potentials of aluminum alloys and those of other metals, are of considerable importance. Furthermore, the solution-potential relationships among the microstructural constituents of a particular alloy significantly affect its corrosion behavior" (Hollingsworth & Hunsicker 1997). The aluminum alloy's predominant metal compositions after aluminum are known by their alloy designations. The four digit alloy groups are as follows:

- 1xxx Aluminum, 99.0% and greater
- 2xxx Copper
- 3xxx Manganese
- 4xxx Silicon
- 5xxx Magnesium
- 6xxx Magnesium and Silicon
- 7xxx Zinc
- 8xxx Other elements
- 9xxx Unused series

The amount of corrosivity of aluminum in a water environment is a factor of water temperature, pH, and percent composition of heavy metals. There are several aluminum alloys that resist corrosion in a water environment and that includes alloy series 1xxx, 3xxx, 5xxx, and 6xxx (Key to Metals 2009).

The drill pipe analysis in this thesis evaluates two alloy series, namely 2xxx and 7xxx. In terms of the corrosive resistance of these alloys, the ASM Corrosion Handbook (Volume 13) outlines the corrosion of each alloy group. The series 2xxx wrought alloys and 2xx.x casting alloy are less resistant to corrosion than other alloy series, specifically those alloys containing a lower percentage of copper (Hollingsworth & Hunsicker 1997). The series designation, such as 2xxx for copper, represents the metal that comprises the greatest mean percentage for that alloy group. Other metals can be present as a lower percentage. For example, a wrought alloy 2xxx which contains lithium has the added benefit of decreasing the density and conversely increasing the modulus of elasticity. One of the early alloys containing lithium was 2020 which was a good structural alloy with strength properties up to 175 °C (350 °F) and a modulus of elasticity "8% higher and a density 3% lower than alloy 7075-T6" (Hollingsworth & Hunsicker 1997, p. 1437-1438).

The series 7xxx wrought alloys and 7xx.x casting alloys contain the greatest mean percentage of zinc. Alloys in this series that are combined with magnesium or both magnesium and copper have different levels of strength. Those alloys with copper have the highest strength. However, copper-free alloys have many desired structural attributes such as "moderate-to-high strength, excellent toughness, and good workability, formability, and weldability" (Hollingsworth & Hunsicker 1997, p. 1437-1438).

The 7xxx wrought and 7xx.x casting alloys are most susceptible to stress-corrosion cracking (SCC). However, the 7xxx series that are copper-free wrought alloys have good corrosion resistance similar to wrought 3xxx, 5xxx and 6xxx alloys. Conversely, 7xxx series alloy with copper, such as "7049, 7050, 7075, and 7178 have lower resistance to general corrosion than those of the same series that do not contain copper. All 7xxx alloys are more resistant to general corrosion than 2xxx alloys, but less resistant than wrought alloys of other groups." (Hollingsworth & Hunsicker 1997, p. 1439)

Current manufactures of ADP both in the 2xxx and 7xxx wrought alloy recommend that the pH of the drilling fluid be maintained between pH 7 to 10 and no higher. That range is consistent for a wide range of drilling fluid types from natural muds with fresh water to gyp-type and lignite based muds (Alcoa 2008, Aluminum Drill Pipe, Inc. 2008).

## 4. MODEL VALIDATION

The temperature model was validated with real world data from a well drilled in Northeastern Iceland in the Bjarnarflag geothermal area, well BJ-15, provided by ISOR, Iceland GeoSurvey, Iceland's premier research institution specializing in geothermal sciences and utilization. The temperature of the standpipe, wellbore diameters, drill pipe diameter, depth of well, drilling fluid circulation losses, formation temperature, drilling duration (well cooling), rock properties, and flow rates inside drill pipe and annulus were input into the model. The model produced a bottom hole temperature that was compared to the MWD (measurement while drilling) recorded data.

The formation temperature of well BJ-15 is quite dramatic as shown below Figure 4:

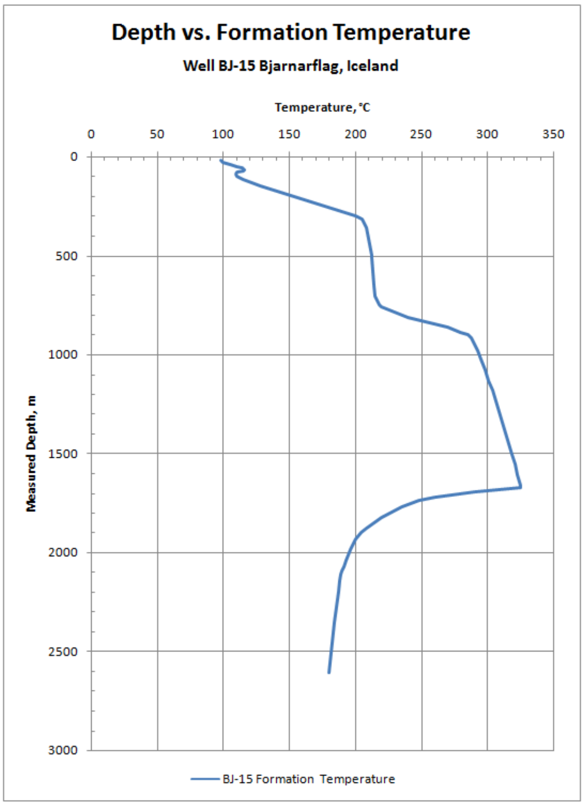


**Figure 4: Well BJ-15 Formation Temperature provided by ISOR.**

The formation temperature drops severely at a depth of 1700 meters since this is below the major aquifer. Therefore the model was tested up to a depth of 1690 meters and the results (temperature outflow) correlated very closely to the recorded fluid outflow temperature. The bottom hole temperature had a percent error less than 25% from the recorded MWD temperature for the random depths tested. To test the margin of error for depths greater than 1700 meters, the model was run to a depth of 1900 meters. The results of all the model runs are shown in Figure 5 below. It is clear that in cases where there is significant cooling in deep geothermal formations, the model cannot accurately estimate the bottom hole temperature that will be encountered during drilling.

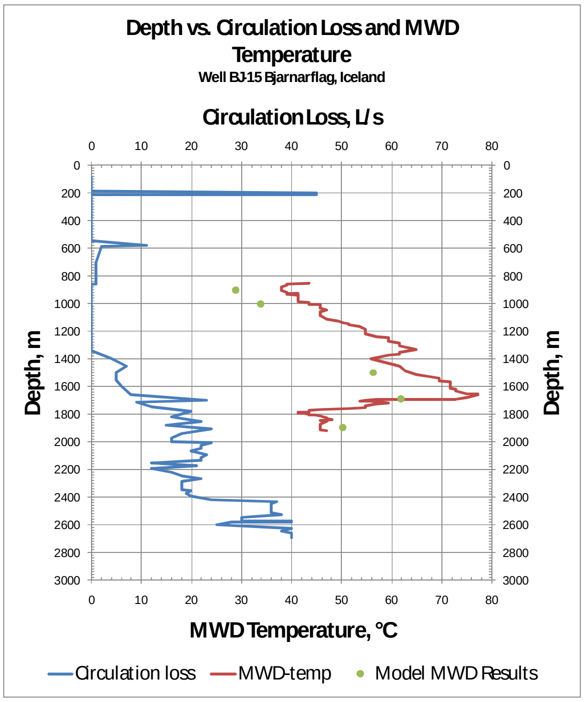


**Figure 5: Model Output for MWD Temperatures versus Actual Data.**

Since the tested wellbore was assumed to have a constant diameter to total depth, it is expected that the model results for the bottom hole temperature will not correlate perfectly to the MWD measurements. Likewise, there are several other minor causes of error including: reservoir formation really follows the BPD more closely than the latest recorded ISOR formation temperature, compared to other historical graphs of the formation temperature of this well; the error between the bottom hole calculations and the MWD recorded data decreases with depth and is therefore more accurate in the more critical areas; generic models take the worse case approach for formation temperature, losses, and surface temp; thermal conductivity of steel drill pipe decreases with increasing temperature. The composition and thermal conductivity of API drill pipe vary from manufacturer to manufacturer and the k-value used in the model was the average thermal conductivity for a similar strength steel for temperatures ranging from 'room temperature' to 600°C; well was modeled as a full diameter 12 ¼ to full depth despite the actual well being drilled with an 8 ½" diameter bit to full depth. Based on the comparison of the temperature model results to the actual data from well BJ-15, the model appears to be a good prediction of the down hole temperatures that will be encountered during drilling and will serve as the method for determining the down hole temperature in wells using ADP.

## 5. ALUMINUM & STEEL DRILL PIPE APPLICATION RANGE

In order to predict the down hole temperature of a well and correlate the yield strength of the ADP at various depths, a model with generic inputs was established. The generic inputs were chosen to be similar to geothermal wells throughout the world and not just those in Iceland. The input were: surface temp, Ts = 20°C, Flow rate up annulus = 50 liter/sec, flow rate inside drill pipe = 50 l/s, formation temperature = Boil Point with Depth curve, drilling fluid =

water, ADP thermal conductivity = 155 W/(m°C). Likewise, the model was designed for the worst possible case in terms of geothermal drilling applications. For example, the formation temperature was assumed to be the boiling point depth curve (BPD) and there were assumed to be no circulation losses within the borehole during drilling. The drilling fluid analyzed during the model runs was pure water despite drilling muds being used throughout most geothermal drilling operations globally. Using water as a drilling fluid was more conservative in terms of the bottom hole temperature prediction since it produced higher temperatures at the bottom of the wellbore compared to mud. The cooling of the well correlated to the drilling days as show in Table 7 and were input into the model for the various test runs. The results of the model using both aluminum and steel drill pipe are shown in Table 8.

**Table 7: Well Cooling Input for Model.**

| Pipe Diameters [m] | Depth [m] | Drilling Days (Circulation time at top) [days] |
|---|---|---|
| | 300 | 9 |
| | 800 | 20 |
| 6 5/8" | 1500 | 30 |
| 5" | 2000 | 40 |
| 4.5" | 2500 | 45 |
| | 3000 | 60 |

**Table 8: Model results of Well bottom temperature for steel and aluminum drill pipes.**

| Model Summary | 6 5/8" Stl | 6 5/8" Al | 5" Stl | 5" Al | 4.5" Stl | 4.5" Al |
|---|---|---|---|---|---|---|
| Depth | $T_t = T_{a\ at\ bottom}$ | $T_t = T_{a\ at\ bottom}$ | $T_t = T_{a\ at\ bottom}$ | $T_t = T_{a\ at\ bottom}$ | $T_t = T_{a\ at\ bottom}$ | $T_t = T_{a\ at\ bottom}$ |
| [m] | [°C] | | | | | |
| 0 | 20 | 20 | 20 | 20 | 20 | 20 |
| 300 | 22 | 24 | 22 | 23 | 22 | 23 |
| 800 | 38 | 50 | 32 | 42 | 32 | 40 |
| 1500 | 80 | 117 | 63 | 94 | 63 | 89 |
| 2000 | 117 | 165 | 91 | 137 | 92 | 131 |
| 2500 | 155 | 209 | 123 | 179 | 125 | 173 |
| 3000 | 186 | 241 | 152 | 213 | 154 | 206 |

The bottom hole temperature at each depth created the temperature envelopes shown graphically in Figure 6 and Figure 7. The temperatures encountered at the bottom of a wellbore during drilling operations differ between steel drill pipe and ADP due to the thermal conductivity of the pipes. ADP has a much higher thermal conductivity and therefore can transfer heat across its boundary much faster. This results in the annulus fluid transferring more heat to the drill pipe fluid, thereby heating the inside drilling fluid faster and resulting in greater down hole temperatures. From this data, the maximum temperature predictions for a well based on depth can be determined and then the appropriate drill pipes can be chosen.

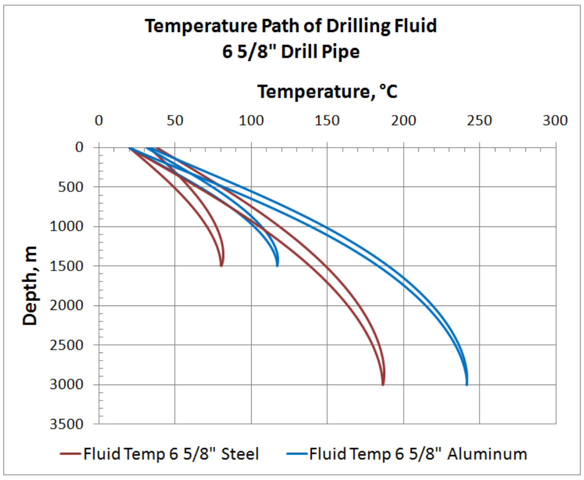


**Figure 6: Temperature Path of Drilling fluid to 1500 and 3000 meters.**

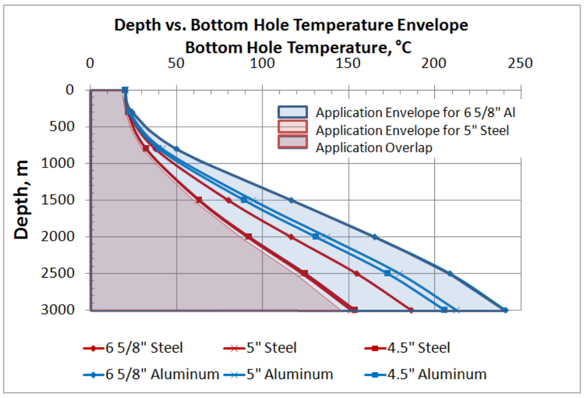


**Figure 7: Depth versus Bottom Hole Temperature for Steel and ADP.**

The use of mud as the drilling fluid results in bottom hole temperatures being significantly lower than temperatures encountered with pure water as a drilling fluid. As mentioned previously, this is due to the lower heat flow rate of mud compared to water. Therefore, as the mud is flowing down the drill pipe, it remains cooler per length of drill pipe compared to water. However, lower heat flow affects the temperature of the mud up the annulus since the mud is slower to conduct the heat from the mud to the borehole wall and the outside wall of the drill pipe. The result of using drilling mud is cooler bottom hole temperatures, but elevated temperature at the surface of the annulus fluid. This would require more mud coolers to reduce the temperature to an appropriate temperature and would further increase the total drilling costs due to excess energy and equipment needed for cooling the drilling mud. A comparison of the temperature predictions for water and mud are shown below in Table 9.

## 6. COMBINED TEMPERATURE & STRUCTURE LIMITS

First, the hook load capacities for several drill rigs are compared to the weight limits of both 5" ADP and 6 5/8" ADP with either a 10 or 20 tonne WOB and to the yield limits of the aluminum alloy. The temperature model predicted the temperature at the bottom of the wellbore as a function of depth. The temperature dependencies of the yield strength of select aluminum alloys have been presented in previous sections. The correlation of depth versus yield strength could then be interpolated between this data. The resulting yield strengths were then converted to a force in tonnes and corrected due to the buoyancy factor. The results are shown in Figure 8 and Figure 9 below and show that the yield strength decreases as depth increases due to the temperature increase with depth.

**Table 9: Comparison of Water versus mud as a drilling fluid and temperature affects.**

| Depth [m] | 6 5/8" Aluminum | | | | | |
|---|---|---|---|---|---|---|
| | Water | | | Mud | | |
| | $T_{t\ at\ 0\ m}$ [°C] | $T_{a\ at\ 0\ m}$ [°C] | $T_t = T_a$ at bottom [°C] | $T_{t\ at\ 0\ m}$ [°C] | $T_{a\ at\ 0\ m}$ [°C] | $T_t = T_a$ at bottom [°C] |
| 300 | 20 | 22.7 | 24.0 | 20 | 22.7 | 21.4 |
| 3000 | 20 | 26.9 | 241.3 | 20 | 41.4 | 138.9 |

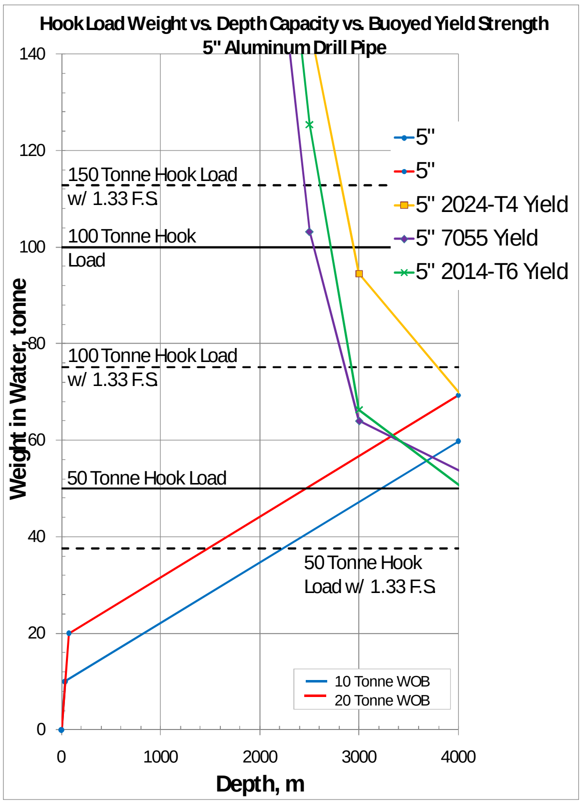


**Figure 8: Aluminum 5" Drill Pipe - Hook Load Weights versus Yield Limits.**

The depth limits based on hook load and yield strength must be corrected for the length of the drill collar. In this analysis, the correction depth for the 20 tonne WOB is 75 meters and for the 10 tonne WOB it is 37 meters. These depths must be added to the depth that corresponds to the intersection of a drill pipe with the yield strength curve.

For example, if one is looking at a WOB of 20 tonnes and using a 5" aluminum alloy 2024 drill pipe, the pipe will reach is yield point due to the weight of the drill string at a depth of 4000 meters. At this depth, a 100 tonne hook load drill rig with a factor of safety of 1.33 applied to the hook load could be used since the yield strength and weight of the pipe do not exceed the hook load capacity of the drill rig.

The yield strength limits that were interpolated from the temperature data were correlated to depth. The Figure 10 below shows the yield strength as a function of depth. The deeper the well goes, the lower its yield strength due to an increase in temperature. Graphs of the ADP application envelopes of depth versus temperature and yield strength could not correctly identify the acceptable area for aluminum drill pipe due to the non-linear behavior of the yield strength of aluminum with temperature.

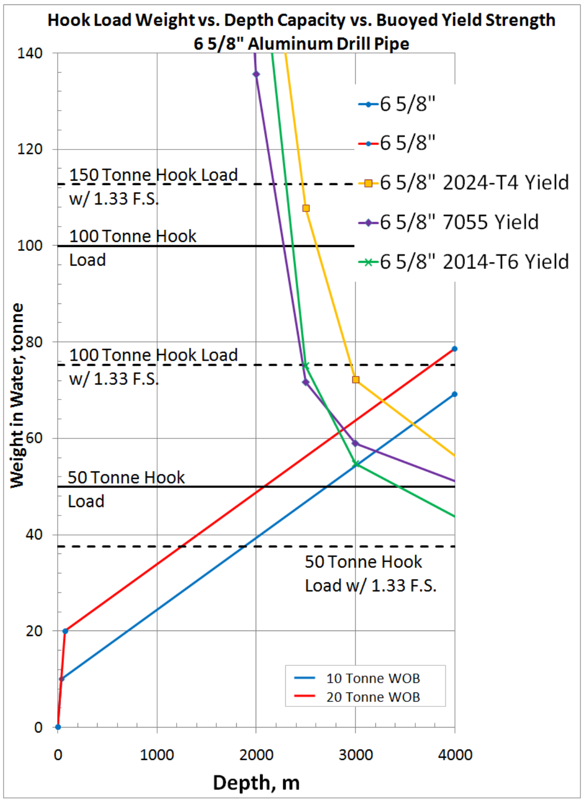


**Figure 9: Aluminum 6 5/8" Drill Pipe - Hook Load Weights versus Yield Limits.**

During drilling, the ultimate torsional yield strength of the pipe reduces as the temperature increases with depth as shown in Figure 11. This figure also shows the maximum allowable applied torque for a drill pipe under axial loads (tension) applied from the weight of the drill string to a depth of 3000 meters. Since the equation to calculate the maximum allowable applied torque depends on the yield strength, the calculations were performed for the yield strength as it changes with temperature. These curves are labeled "Torque w/ Tension". Lastly, the allowable torque for drill pipe under a tension load due to 3000 meters of drill string was plotted at room temperatures to compare the steel grades to the aluminum grades. For instance, if a 3000 meter wellbore has a bottom hole temperature of 200°C, the maximum allowable torque applied to the top drill pipe of a 3000 meter long drill string is 1000 daN.m for aluminum alloy 2024-T4. The maximum allowable limits for a 3000 meter well have been plotted on that graph to show where it would intersect the yield curve and the maximum temperature that may be encountered before the drill pipe begins to yield. For example, a 5" diameter aluminum alloy drill pipe of grade 2014-T6 with an applied tension load for a well depth of 3000 meters would begin to yield at approximately 100°C with an applied maximum allowable torque of approximately 4090 daN.m. If the applied torque were reduced, it can be seen that the temperature limit increases.

## 5. COST ESTIMATE

In addition to structural and performance benefits of ADP, there are resulting cost advantages. However, due to the variability of drilling performance from location to location

– including geologic conditions, well specifications, equipment variability, contractor experience, etc – general cost estimates are difficult to ascertain and cannot be accurately calculated due to the lack of transparent historical geothermal drilling cost data.

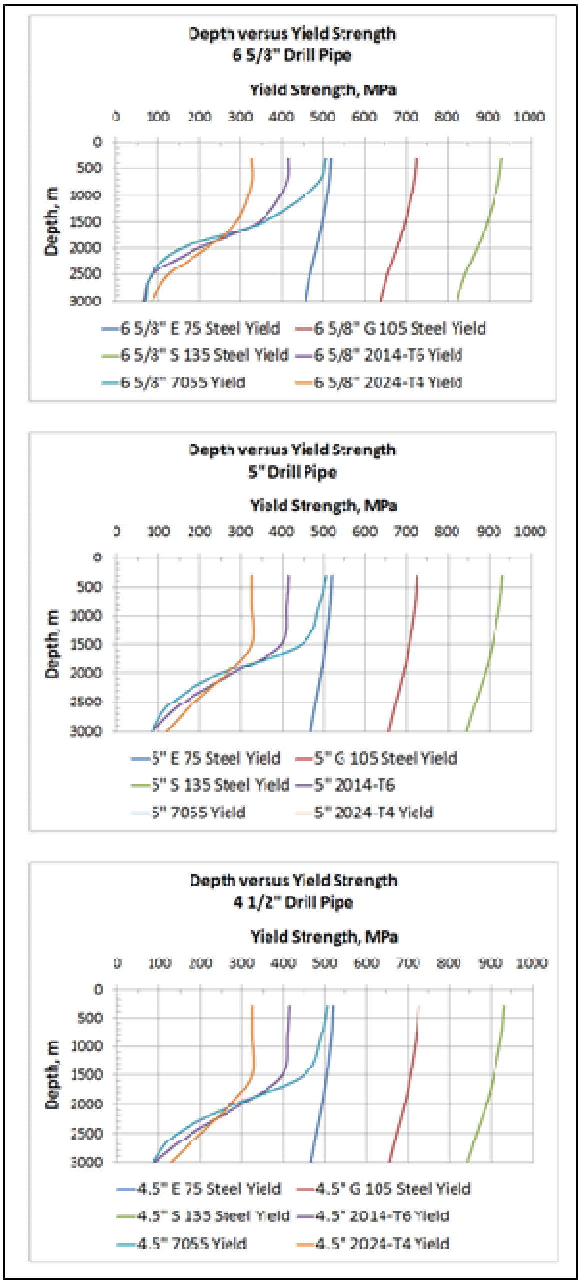


**Figure 10: Depth versus Yield Strength for 6 5/8”, 5”, & 4.5” Drill Pipe.**

## 5.2 Rig Hook Load Comparison and ADP Price per Meter

The structural benefits of aluminum alloy drill pipe were shown in the above analysis. The result is a superior product at a third of the weight of steel which then helps to achieve greater depths with smaller drill rigs. In a drilling project in Western Siberia, the use of aluminum drill pipe allowed a 125-ton Uralmash drill rig to achieve a total depth (TD) of 4,200 meters. Comparatively, using steel drill pipe to that depth would require the use of a 250 ton drill rig. In other words, the maximum depth achieved by a 125-ton drill rig using steel drill pipe would be 2,500 meters or, at best, 2,700 meters (Chesnokov 2008).

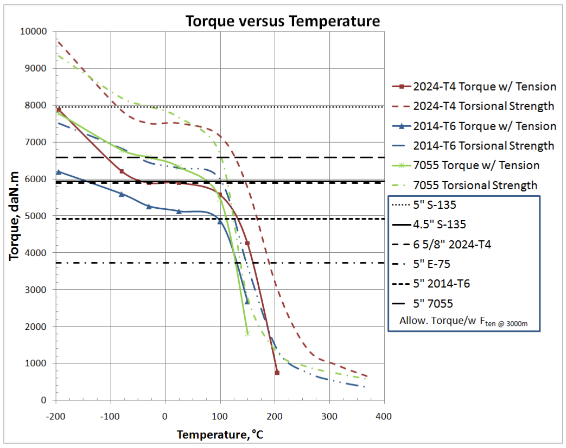


**Figure 11: Torque Strength as a function of Temperature.**

Two drill rigs with different hook load ratings have been analyzed. The cost per day and days of drilling are approximations based on limited data. The first cost analysis is a lump sum analysis and considers the fuel cost saving encountered with the use of ADP compared to steel drill pipes. The ratio of the engine power needed to supply the drilling fluid at the required pressure for ADP versus steel drill pipe was used as a reduction for the fuel costs. The engine power required for the pump was determined with a pump efficiency of 0.87 divided by the results of the power required due to pressure losses, as shown in Table 10.

**Table 10: Power Requirements of Engine for Mud Pumps.**

| **Engine Power Required** | | **Steel Drill Pipe** | | **Aluminum Drill Pipe** | |
|---|---|---|---|---|---|
| Efficiency = | 0.87 | Steel 5" kW | Steel 4.5" kW | AA 6 5/8" kW | AA 5" kW |
| Newtonian | | 946 | 1351 | 519 | 1075 |
| Non-Newtonian | | 895 | 1266 | 504 | 1014 |

The ratio of the engine power of the 6 5/8” ADP to the 5” steel was 55%. This reduced the total fuel cost that would be expected when using steel drill pipe. The results of the lump sum cost analysis are shown in Table 11. The cost per day for the rigs is an indicative price since the current drilling day rates are highly erratic. The simple lump sum compares the cost per day for a 200 tonne and 100 tonne rig and a stated number of drilling days. This first method is independent of the well depth. The use of aluminum drill pipe produced a fuel savings cost of approximately 8% of the total cost of the well.

The second cost estimate calculates the difference between the rig and fuel requirements for a well 3000 meters deep and compares a 5” steel drill pipe with a 6 5/8” ADP. Referring to Figure 12 below, with a 10 tonne WOB and a depth of 3000 meters, the proper hook load limits were determined. For the 6 5/8” ADP of alloy 2024-T4 which is below the yield strength limits, a 100 tonne hook load with a factor of safety of 1.33 can be used. For the 5” steel drill pipe, the weight of the steel exceeds the 100 tonne hook limits but falls within the 150 tonne hook load limit with a 1.33 factor of safety. However, 30% will be added to the hook loads for a directional well. Therefore, a 200 tonne and 150 tonne hook load was analyzed. The steel and aluminum points are the intersection of the 10 WOB line with the depth of 3000m. The same 30% safety factor was applied to this point to get the weight of the drill string, with both steel and aluminum drill pipe, in a directional well. Table 12 compares the cost of a 3000 meter deep well for both a steel drill pipe and an aluminum drill pipe. Here the savings of using ADP are quite apparent, with total savings of $558,000. These savings are due to both the reduction in energy for the mud pump and the utilization of a reduced hook load drill rig, with longer drilling days but reduced daily rig rates as compared to the steel drill pipe case. The total well costs for drilling to a depth of 3000 meters was checked relative to historical data and was found to be in the range of the well cost data provided in the MIT Geothermal report (2006). The MIT data showed that for a well of 3000 meters the costs are in the range of $2 to $4 million dollars (in 2004 US$). Therefore, the values estimated with this cost estimate are within an acceptable range. This rough cost estimate, results in a cost of $1228/meter for ADP compared to $1400/meter for steel as calculated for a 3000 meter deep well with varying drilling days.

These cost estimates neglect the actual cost of the aluminum and steel drill pipe. The costs for aluminum drill pipe vary anywhere from 1.5 to 2 times the cost of steel drill pipe (Chandler et al 2006, Jellison 2007). Yet Chesnokov (2008) reports that while “a ton of pipes fabricated from aluminum alloy is approximately 30-40 percent more expensive than a ton of steel pipes”, the price per meter of ADP is actual equal to or sometimes less than that of steel. ADP marketing brochures report a higher initial cost of ADP compared to steel drill pipe, but tout substantial savings in operating costs with the use of ADP. The scarcity of aluminum drill pipes on the markets (outside of Russia) has an effect on the prices as a higher demand would reduce and stabilize the costs.

**Table 11: Lump Sum Cost Analysis.**

| Method 1: Cost Analysis - Lump Sum | | | |
|---|---|---|---|
| | 200 Tonne Rig | 100 Tonne Rig | |
| Cost per Day ($) | 35,000 | 25,000 | |
| Drilling Days | 45 | 55 | |
| % of Rig costs to Total Cost | 50.0% | 50.0% | |
| Total Well Cost | $3,150,000 | $2,750,00 0 | |
| Fuel Cost (% of total cost) | 18% | 18% | 1 |
| Fuel Cost Total | $567,000 | $495,000 | |
| Pumping Power Reduction Ratio 5" to 6 5/8" | 54.9% | 54.9% | |
| Fuel Cost | $311,270 | $271,743 | |
| Savings | $255,730 | $223,257 | |
| % of Fuel Savings | 8.12% | 8.12% | |

[1] From correspondance with Sverrir Thorhallsson, Head of Engineering Dept., ISOR Iceland GeoSurvey

## 6. CONCLUSION

In conclusion to this analysis, the current production of ADP is capable of being deployed and tested in the geothermal drilling industry. The temperature model produced the most severe and therefore most conservative results for the bottom hole temperatures that the aluminum drill pipe would experience for the general inputs that were used. Through testing the model with various inputs, it was determined that water as a drilling fluid produced the greatest down hole temperatures; the use of the BPD curve is the critical maximum for single fluid phase geothermal wellbores; the absence of the loss of circulation from the annulus maintained the high down hole temperatures; and a higher temper thermal conductivity resulted in more heat transfer per meter than other values.

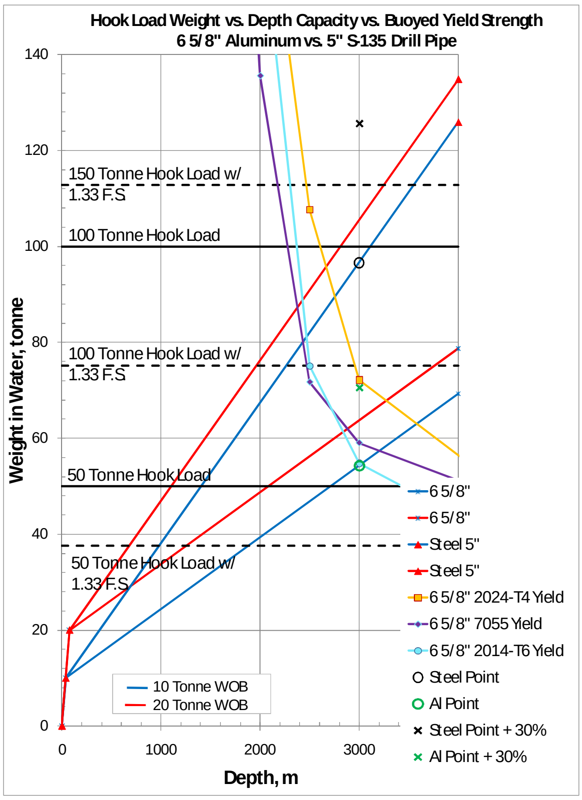


**Figure 12: Hook Load Limits at 3000m for Steel versus Aluminum.**

**Table 12: Method 2 – Cost Analysis comparing 3000m Steel vs. ADP well.**

| Method 2: Cost Analysis - Reduction Elements | | | |
|---|---|---|---|
| | 5" Steel | 6 5/8" ADP | |
| Rig Limit for 3000 meter | 200 tonne | 150 tonne | |
| Cost per Day ($) | 35,000 | 27,500 | 1 |
| Drilling Days | 60 | 67 | 1 |
| % of Rig costs to Total Cost | 50.0% | 50.0% | |
| Sub Total Well Cost | $4,200,00 0 | $3,685,00 0 | |
| Pumping Power Required (kW) | 823.11 | 451.87 | |
| Engine Efficiency | 0.87 | 0.87 | |
| Required Engine Power (kW) | 946 | 519 | |
| Drilling Days | 60 | 67 | |
| Specific Oil Consumption l/kWh | 286 | 156 | 2 |
| Pumps at full power | 45% | 45% | |
| Total Consumption (L) | 185328 | 112882 | |
| Price per liter (Diesel) | $0.596 | $0.596 | 3 |
| Total Fuel cost | $110,455 | $67,277 | |
| % Difference in Fuel Costs | 48.6% | | |
| % Difference in Total Costs | 13.1% | | |
| Total Rig and Fuel Savings for ADP | $558,178 | | |
| Price per meter | $1,400 | $1,228 | |

[1] From correspondance with Sverrir Thorhallsson, Head of Engineering Dept., ISOR Iceland GeoSurvey

[2] Data from Cummins Power Generation for Diesel Generators

www.cumminspower.com/www/common/templatehtml/technicaldocument/SpecSheets/Diesel/na/d-3425.pdf

[3] Price based on 2/3/09 EIA Spot Prices for NY Harbor No. 2 Diesel - cents/gal of 133.55

EIA Retail Price 2/2/09 = 225.6 cents/gal

http://tonto.eia.doe.gov/dnav/pet/pet_pri_gnd_dcus_nus_w.htm

The applied stresses were calculated for the drill pipe and compared to the increased temperatures encountered in geothermal wells. The yield strength was correlated to depth and the yield limits for the tested grades of drill pipe should be limited by these values. The non-linear degradation of aluminum alloys versus temperature, in combination with the non-linear bottom hole temperature with depth, make a straight correlation difficult to illustrate. The torque applied to most drill pipes is limited to 80% of the tool joint make-up and the applied torque from the top drive rarely exceeds 3000 daN·m. Based on the results, the AA 7055, 2014, and 2024, can operate safely up to temperatures of 140°C, 150°C and 190°C respectively.

The hook loads for a 5” diameter pipe with a 20 tonne WOB, the depth limit for both the 2014 and 7055 alloy was roughly about 3475 meters with the correction depth included. The ADP with a 10 tonne WOB can be utilized to a depth of approximately 3740 meters for 2014 and 7055 alloys, again with the correction factor included. The 5” diameter pipe of aluminum alloy 2024 can be used to depths greater than 4000 meters. As the diameter of the pipe increases, the depth limits decrease. The 6 5/8” diameter pipe with a 20 tonne WOB has depth limits of about 2900 meters for both the 2014 and 7055 alloys, and a limit of around 3325 meters for 2024 alloy. The 10 tonne WOB for that diameter can reach depths of nearly 3040, 3240, and 3640 meters for alloy grades 2014, 7055, and 2024 respectively.

Analysis of the bending stresses with depth compared to the yield strength with temperature showed that the stresses applied to the ADP for an incline angle of 1.4° are significantly under the yield curves for temperatures up to 300°C.

The internal yield pressure or burst strength for aluminum alloy 7055 and 2014 are adequate to a depth of 4000 meters when the bottom hole temperature does not exceed ≈ 130°C. The aluminum alloy 2024 has a lower yield strength, which reduces the operating depth to 3500 meters with a bottom hole temperature below ≈ 120°C.

The culmination of all the structural stresses applied to the drill pipe gives rise to the fatigue stresses. The estimation of fatigue stresses and the initiation of fatigue failure are highly complex and variable stresses differ between wells and drill rigs. This phenomenon affects both steel and aluminum drill pipes and continues to be at the core of drill string analysis and improvements.

The structural analysis and strength calculations were tested for various scenarios to determine the critical location of the drill pipe for the various stresses. The tension or axial forces were calculated for the top pipe since this was both the maximum tensile load on any other drill pipe and this resulted in yield strength failures for temperatures up to 150°C. When a pipe at a depth of 2500 meters was analyzed for a total well depth of 3000 meters, the axial force was reduced and the temperature limits increased to 260°C for aluminum alloys 2024 and 7055, and increased to 205°C for alloy 2014. While analyzing a pipe at a depth of 2500 meters, the torsional stresses increased despite the tension forces decreasing. The increase, however, did not exceed the pipe limits.

ADP reduces the pressure losses, therefore reducing pump energy and fuel costs. The decreased weight per meter as compared to steel, allows ADP to reach greater depths with small hook load rated drill rigs. The continued engineering of aluminum alloys is critical to geothermal drilling and will only enhance and improve the current benefits of ADP and increase the temperature limits. This will only serve to help the geothermal industry to drill faster, deeper wells; thereby bringing wells online faster, decreasing the time to provide power to customers, and reducing the costs through economies of scale. ADP is an important technology to help the geothermal industry compete financially with base load fossil fuel power plants.

## REFERENCES


Alcoa 2008, ‘Drill Pipe Engineering Data –Version 1.0’, Alcoa Oil and Gas Brochure, viewed 30 Aug 2008, < http://www.alcoa.com/oil_gas/en/home.asp>.

The Aluminum Association 2006, International Alloy Designations and Chemical Composition Limits for Wrought Aluminum and Wrought Aluminum Alloys, The Aluminum Association, Arlington, VA.

Aluminum Drill Pipe, Inc. 2008, ‘Brochure’, Aluminum Drill Pipe, Inc. viewed 28 Dec 2008, <http://aluminumdrillpipe.com/Brochure.web.pdf>

Aquatic Company 2008, Aquatic Company, viewed 12 January, 2008, < http://www.aqua-co.com/eng/products/adp1.shtml>

Bird, R.B., Stewart, W.E. & Lightfood E.N.: Transport Phenomena, 2nd edn, 2002, John Wiley & Sons, Inc., New York.

Bourgoyne, A.T., Millheim, K.K., Chenevert, M.E. & Young, F.S.: Applied Drilling Engineering, 1991, Society of Petroleum Engineers, Texas.

Chandler, R.B., Jellison, M.J., Payne, M.L. & Shepard, J.S.: Advanced and emerging drillstring technologies over operational challenges, *World Oil*, **October**, (2006), 23-34.

Chesnokov, Alexei: Weatherford’s “Aquatic” Spreads the Gospel of Aluminium for Drilling Deep On and OffShore, *Oil & Gas Eurasia*, **October**, (2008), http://www.oilandgaseurasia.com/articles/p/87/article/744.

Chugunov, V, Fomin, S & Hashida, T: Heat Flow Rate at a Bore-Face and Temperature in the Multi-Layer media Surrounding a Borehole, *International Journal of Heat and Mass Transfer*, **46**, (2003), 4769-4778.

Fomin, S, Hashida, T, Chugunov, V & Kuznetsov, A.V.: A Borehole Temperature During Drilling in a Fractured Rock Formation, *International Journal of Heat and Mass Transfer*, **48**, (2005), 385-394.

Gelfgat, Y.A., Gelfgat, M.Y., & Lopatin, Y.S. 2003, Advanced Drilling Solutions: Lesson from the FSU, vol. 1, PennWell, Oklahoma.

Hefu, H 2000, Study on Deep Geothermal Drilling Into a Supercritical Zone in Iceland, *United Nations University Geothermal Training Programme Reports*, **7**, (2000), 105-137.

Hollingsworth, EH & Hunsicker, HY: Corrosion of Aluminum and Aluminum Alloys. In: ASM Handbook

Volume 13 Corrosion (electronic version), 1997, ASM International.

Jellison, M: Drill Pipe and Drill Stem Technology, *Drilling Contractor*, March/April, (2007), 16-22.

Kanev, K, Ikeuchi, J, Kimura, S & Okajima Atsushi: Heat Loss to the Surrounding Rock Formation from a Geothermal Wellbore, *Geothermics*, **26**, (1997), 329-349.

Keys to Metals 2009, ‘Corrosion of Aluminum and Aluminum Alloys’, Key to Metals: Nonferrous, viewed 25 Jan 2009, < http://nonferrous.keytometals.com/default.aspx?ID=CheckArticle&NM=14>

Miscow, G.F., deMiranda, P.E.V., Netto, T.A. & Placido, J.C.R.: Techniques to characterize fatigue behaviour of full size drill pipes and small scale samples, *International Journal of Fatigue*, **26**, (2004), 575-584.

Moore, PL 1986, *Drilling Practices Manual*, 2edn, PennWell Books, Tulsa, Oklahoma.

Rahman, M.K., Hossain, M.M., & Rahman, S.S.: Survival assessment of die-marked drill pipes: integrated static and fatigue analysis, *Engineering Failure Analysis*, **6**, (1999), 277-299.

Santoyo, E., Garcia, A., Espinosa, G., Santoyo-Gutiérrez, S. & González-Partida: Convective heat-transfer coefficients of non-Newtonian geothermal drilling fluids, *Journal of Geochemical Exploration*, **78-79**, (2003), 249-255

U.S. Department of Energy 2006, The Future of Geothermal Energy: Impact of Enhanced Geothermal Systems (EGS) on the United States in the 21st Century, Massachusetts Institute of Technology, Boston.

Vaisberg, O, Vincke, O, Perrin, G, Sarda, J.P., & Fay, J.B.: Fatigue of Drillstring: State of the Art, *Oil & Gas Science and Technology*, **57**, (2002), 7-37.